

COMPUTATION OF OCCUPANT EXPOSURE IN AN OFFICE CUBICLE

H. Ezzat Khalifa^a, Samuel J. Prescod^b, John F. Dannenhoffer III^c

Syracuse University, Syracuse, NY

Basman Elhadidi^d

Cairo University, Giza, Egypt

ABSTRACT

A Computational Fluid Dynamics (CFD) model for exposure calculations was developed for an occupant in a typical office cubicle. A commercial CFD code was employed, along with the widely-used and readily accessible $k-\varepsilon$ turbulence model. By simplifying the seated occupant model to an assembly of simple blocks representing the torso, thighs and legs, it was possible to simulate a realistic cubicle and its occupant with an intermediate grid of $\sim 100,000$ structured cells. This allowed the model to run on a single high-end PC, and made it a practical alternative to the well-mixed zonal models that ignore spatial gradients. The model was used to study the effect of realistic office cubicle environments with multiple emitting surfaces (*e.g.*, panel partitions, desks, carpet, computer), and the occupant in different positions. The effects of four important factors on the normalized breathing zone contaminant concentration were analyzed: 1) the effect of various manikin representations, 2) the effect of various supply diffuser locations, 3) the effect of shifting the manikin (left, right and back), and 4) the effect of the manikin orientation (facing computer and facing wall). The present CFD model indicates that the spatial non-uniformities, even in a room ventilated with a mixing-ventilation system, could result in as much as 45% difference in exposure compared with the calculations based on the simpler, well-mixed assumption. Furthermore, the results of the present model could be used to correct the predictions of the simpler well-mixed, zonal models for spatial non-uniformities, and for the effects of the person's position within the cubicle or the supply diffuser location. This would allow a higher-fidelity assessment of exposure in the office environment. The simple CFD approach is particularly valuable for exposure assessment with displacement and personal ventilation systems, which produce steeper gradients in velocity, temperature and concentration within the occupied space.

^a Professor, Mechanical & Aerospace Engineering, and Director, STAR Center for Environmental Quality Systems.

^b Currently at M.S. Kennedy Corporation, Liverpool, NY

^c Associate Professor, Mechanical & Aerospace Engineering.

^d Assistant Professor, Aeronautical Engineering

INTRODUCTION

Computational models used for predicting human exposure to indoor pollutants typically fall into two categories: zonal and computational fluid dynamics (CFD). Zonal models divide the space into zones (rooms, hallways, etc) and treat a zone as a well mixed space characterized by a single temperature and a single concentration value for each contaminant present (same as the exhaust values), *i.e.*, they do not take into account the spatial non-uniformities in the flow, temperature and concentration present in ventilated spaces, even in those served by mixing ventilation systems. Examples of these models include EXPOSURE¹, RISK², IAQX³, I-BEAM⁴, the National Institute of Standards and Technology's (NIST) CONTAMW⁵, and Lawrence Berkeley National Laboratory's (LBNL) COMIS⁶. We add to those the IAQ feature included in the MEDB-IAQ⁷ database of Zhang *et al.* EXPOSURE, RISK and MEDB-IAQ utilize experimentally determined material VOC emission data to estimate the concentrations of pollutants in the room (the same data could also be input to CONTAMW and COMIS). They are designed for ease of use and fast assessment of exposure to VOC contaminants using the species mass balance equation. CONTAMW and COMIS are multi-zone models that allow the simulation of contaminant distribution within a multi-room, multi-zone building represented as a flow network of interconnected nodes (each node is a well-mixed zone). The inter-zonal flow occurs through door openings, cracks and ducts. Because of their simplicity, these models allow the study of time-dependent events, such as a contaminant release.

To capture the spatial gradients within the occupied space and, especially, within the personal microenvironment (PME) closest to the human body, CFD programs must be employed. CFD models are computationally-intensive tools that require the numerical solutions of the full complement of transport partial differential equations (at least five equations, plus as many additional equations as the number of contaminant species, and typically 2 more equations to describe turbulence). Notable CFD investigations of the non-uniform conditions in the PME include the work of Murakami, *et al.*^{8,9,10}, Nielsen *et al.*^{11,12}, Topp *et al.*^{13,14,15}, Hayashi *et al.*^{16,17}, Ito, *et al.*¹⁸, and Omori *et al.*¹⁹. Typically, these studies use intermediate grids of a few hundred thousand cells and the popular 2-Equation k - ϵ turbulence model (or its low Re variant). To avoid the use of a densely-packed grid near the surfaces, these efforts often employ the wall-function approach (see Versteeg *et al.*²⁰). Some of the Murakami and Kato publications cited above include both cyclic and constant flow inhalation, and therefore account for the interaction between the PME and the respiration air in the breathing zone (BZ).

Recently, as part of a parallel effort to the one described in this paper, Sideroff *et al.*^{21,22} developed detailed CFD models of the flow around an anatomically-accurate thermal manikin using unstructured fine grids (millions of cells), and compared the computational results with the mixing and displacement ventilation benchmark cases of Nielsen *et al.*¹¹. However, the room representation in Sideroff's analysis was intentionally made very simplistic to match Nielsen's experimental benchmark cases (essentially a wind tunnel with a seated or a standing manikin). Furthermore, these benchmark cases did not include contaminant sources at the walls or floor, nor did they include office components such as wall panels, desks, cabinets, computers, etc, which have been shown to be major sources of contamination²³. Sideroff's analysis required extensive computing resources (days per run on a Beowulf parallel computer cluster). Such resources would be prohibitive for practical IAQ calculations and are rarely available outside research organizations. The inclusion of realistic office cubicle representations would have made

a calculation of exposure at the level of detail employed by Sideroff *et al.*^{21,22} even more prohibitive. While such fine detail is necessary to capture thermal and contaminant transport from sources within the PME, it is not obvious that this will be necessary to compute reasonably accurate exposure to contaminants entering the room with ventilation/infiltration air, or emitted from surfaces far from the PME (*e.g.*, walls, furniture, etc).

This paper summarizes a study of occupant exposure in a typical office cubicle, using CFD simulations that can be performed using commercial CFD codes, running on a typical high-end single-processor PC platforms.

ANALYSIS METHODOLOGY

In this study two versions of commercial CFD software were employed, AIRPAK and FLUENT²⁴ (A/F). AIRPAK is a derivative of FLUENT tailored for indoor airflow computations. To guide the selection of the appropriate level of grid simplification and turbulence model, and to check the quality of the simpler CFD approach, we compared its carpet and wall contaminant distributions with those of the much more refined models employed by Sideroff *et al.*²¹, using Nielsen's benchmark geometry and boundary conditions¹¹. This was followed by an analysis of contaminant distributions within a typical office cubicle with emitting partition walls, furniture, carpet and computer (see Fig. 3 below). Three simple manikin representations consisting of an assembly of heated blocks were created and embedded in the cubicle opposite the computer (also represented by a heated block). CFD analyses were performed to obtain the spatial distributions of emissions from the carpet, furniture, partitions and computer with various occupant locations/orientations, air diffuser locations and flow rates.

As an indication of exposure, the concentration of the selected contaminant was averaged in a small BZ volume (a 2x2x2 cm volume at the nose location: $y = 1.1$, $z = 0.6$, $0 < x < 2.44$ m). Because the species conservation equations are linear in the concentration, the calculations can be computed for arbitrary emission rates (per unit area of surface) and scaled to match the actual measured rates²³. Absent contaminant filters and adsorption of the emitted contaminants within the cubicle, the emission rate is equal to the contaminant exhaust rate, which is also equal to the uniform concentration that would have been computed by a well-mixed zonal model like RISK. Therefore,

$$C_a = C_m \cdot EF_a / EF_m, \quad (1)$$

where C_a is the actual concentration in the BZ corresponding to the actual emission factor²³ EF_a , and C_m is the concentration in the BZ predicted by the A/F model corresponding to the assumed emission factor EF_m . Because it is more convenient in A/F to impose a concentration boundary condition rather than a flux boundary condition (an emission factor), the EF_m was computed from the exhaust concentration, the exhaust air flow rate and the area of the emitting surface as follows:

$$EF_m = 10^9 \cdot C_e \cdot m_e / A, \quad (2)$$

in which EF_m is the model emission factor in $\mu\text{g}/\text{h}\cdot\text{m}^2$, C_e is the exhaust concentration (mass fraction), m_e is the exhaust mass flow rate (kg/h), and A is the emitting surface area (m^2).

Therefore, Equation (1) can be written as:

$$C_a = 10^{-9} (C_m/C_e) \cdot EF_a \cdot A / m_e. \quad (3)$$

Exposure in a given period of time can be estimated by multiplying the above concentration by the amount of air inhaled during the same period. Equation (3) suggests that a convenient way of expressing the results of the A/F CFD model is to normalize all concentrations of a contaminant in the cubicle by the exhaust concentration of the same cubicle. Since the exhaust concentration also corresponds to the uniform value obtained by a zonal, lumped-parameter (well-mixed) model at the same emission and ventilation rates, the normalized concentrations provide a direct comparison between the CFD calculations of the non-uniform concentration field and the zonal calculations of a uniform value.

Case Designation

Each case is designated by a string of alpha-numeric characters signifying, from left to right: a) the maximum height of the first grid point from a surface; b) the grid stretch ratio (how tightly packed is it near a surface, the smaller the tighter the grid near the surface); c) the maximum allowable grid size; d) the turbulence model (K for standard $k-\varepsilon$, R for *RNG* $k-\varepsilon$, and O for the zero-equation model²⁵); e) the type of wall function used (S for standard, E for enhanced, and N for N/A); f) the location of the manikin (N for nominal, L for shifted 0.3 m to the left, R for shifted 0.3 m to the right, B for shifter 0.3 m backward); and g) is for manikin orientation (F for facing forward and W for facing the wall).

COMPARISON WITH DETAILED CFD MODELS

We compared the results using coarse and intermediate grids and 2-Equation turbulence models (standard $k-\varepsilon$ and *RNG* $k-\varepsilon$) with the fine grid computations of Sideroff *et al.* Two test cases were considered, (i) a uniform floor emission source, and (ii) a uniform wall emission source. A total of 17 combinations (Table 1) of grid refinement, turbulence models and wall treatment were analyzed and compared with 3 calculations based on Sideroff's detailed, fine-grid benchmark flowfields, referred to here as BM SKE, BM V2F and BM New V2F for, respectively, the standard $k-\varepsilon$ (with enhanced wall functions: EWF), baseline v^2-f and a revised v^2-f with improved resolution near the emitting surfaces. The revised v^2-f run brought the y^+ values (see Versteeg *et al.*²⁰) down to $\sim O(1)$ as they are around the manikin. In Sideroff's baseline run, the y^+ values for the first cell adjacent to the floor and side walls were comparable to, and sometimes higher than those used in the present intermediate-grid studies ($y^+ \sim 5-10$). In all the cases studied in this validation exercise, the manikin was located at the nominal position (0.7m from inlet) and facing forward (e.g., Case 501005ONNF designates an essentially uniform grid (5cm spacing in x, y and z directions), employing the 0-Equation turbulence model (no wall functions); whereas case 101210RENF designates a case with a tighter, finer grid ($\sim 443,000$ grid points), using the *RNG* $k-\varepsilon$ turbulence model and the enhanced wall functions.

For the floor contaminant, the contaminant was emitted from the floor by specifying a uniform CO_2 mass fraction of 10^{-5} at the floor. Figure 1 is an example of these comparisons, depicting the floor contaminant normalized concentration along a vertical line passing through the BZ. The solid lines represent Sideroff's fine-grid solutions, the solid symbols represent the $k-\varepsilon$ cases listed in Table 1, and the open symbols represent their *RNG* counterparts. It can be seen that there is a significantly bigger difference between the various turbulent models and their associated near-wall treatment than between the various grids with the same turbulence model. This highlights

the significance of selecting the appropriate turbulence model and characterizing the turbulence boundary conditions. Figure 1 shows that the Standard $k-\varepsilon$ model with the SWFs (solid symbols) is closest to Sideroff's v^2-f computations, and that grid refinements have a relatively small effect on normalized BZ concentration ($\sim 10\%$). This may indicate that grid convergence with the simplified manikin geometry is achieved relatively quickly due, in part, to the fact that the simplified manikin, whose facets are parallel to either x, y or z, allows the use of a simpler, structured, essentially Cartesian grid.

Table 1. Cases Studied in the Comparison with Sideroff *et al.*²¹

Case	Max Init Height, cm	Stretch Ratio	Max Grid Size, cm	Turbulence Model	Wall Function	Manikin Location	Manikin Orientation	Grid Points
102010KSNF	1.0	2.0	10.0	Std $k-\varepsilon$	Std	Nominal	Fore	87805
101510KSNF	1.0	1.5	10.0	Std $k-\varepsilon$	Std	Nominal	Fore	167235
101210KSNF	1.0	1.2	10.0	Std $k-\varepsilon$	Std	Nominal	Fore	442656
201510KSNF	2.0	2.0	10.0	Std $k-\varepsilon$	Std	Nominal	Fore	56779
201510KSNF	2.0	1.5	10.0	Std $k-\varepsilon$	Std	Nominal	Fore	77554
101210KSNF	2.0	1.2	10.0	Std $k-\varepsilon$	Std	Nominal	Fore	160167
501005KSNF	5.0	2.0	10.0	Std $k-\varepsilon$	Std	Nominal	Fore	58800
101210KENF	1.0	1.2	10.0	Std $k-\varepsilon$	Enh	Nominal	Fore	442656
102010RSNF	1.0	2.0	10.0	RNG $k-\varepsilon$	Std	Nominal	Fore	87805
101510RSNF	1.0	1.5	10.0	RNG $k-\varepsilon$	Std	Nominal	Fore	167235
101210RSNF	1.0	1.2	10.0	RNG $k-\varepsilon$	Std	Nominal	Fore	442656
202010RSNF	2.0	2.0	10.0	RNG $k-\varepsilon$	Std	Nominal	Fore	56779
201510RSNF	2.0	1.5	10.0	RNG $k-\varepsilon$	Std	Nominal	Fore	77554
201210KSNF	1.0	1.2	10.0	RNG $k-\varepsilon$	Std	Nominal	Fore	160167
501005RSNF	5.0	1.0	5.0	RNG $k-\varepsilon$	Std	Nominal	Fore	58800
101210RENF	1.0	1.2	10.0	RNG $k-\varepsilon$	Enh	Nominal	Fore	442656
501005ONNF	5.0	1.0	5.0	0-Eqn.	N/A	Nominal	Fore	58800

The results for the side-wall emissions (Fig. 2) showed similar trends, namely: there is a stronger influence on the normalized concentration of the turbulence model and the near wall treatment (wall function) than of the grid refinement (ranging from 57,000 to 443,000 grid points in these computations). The differences in BZ normalized concentration for a given turbulence model and associated wall function is typically less than 10% for the wide range of grids investigated.

Given these results, we judged the standard $k-\varepsilon$ turbulence model with SWFs and intermediate grids ($\sim 100,000$) to be satisfactory for conducting the sensitivity analyses reported in the remainder of this section. This is quite manageable on typical high-end single processor PCs that are accessible to most IEQ practitioners, and is in line with the work of Murakami, Kato and their collaborators, and Srebric and her collaborators^{26,27,28}. However, it was not possible categorically to disqualify other turbulence models and near-wall treatments (*e.g.*, the RNG $k-\varepsilon$ with EWFs) because of the lack of benchmark concentration data. This highlights the needs for detailed benchmark data of not just the velocity and temperature distributions, but also the concentration distribution.

Figure 1. Normalized Concentration of Floor Contaminant from Floor to Ceiling

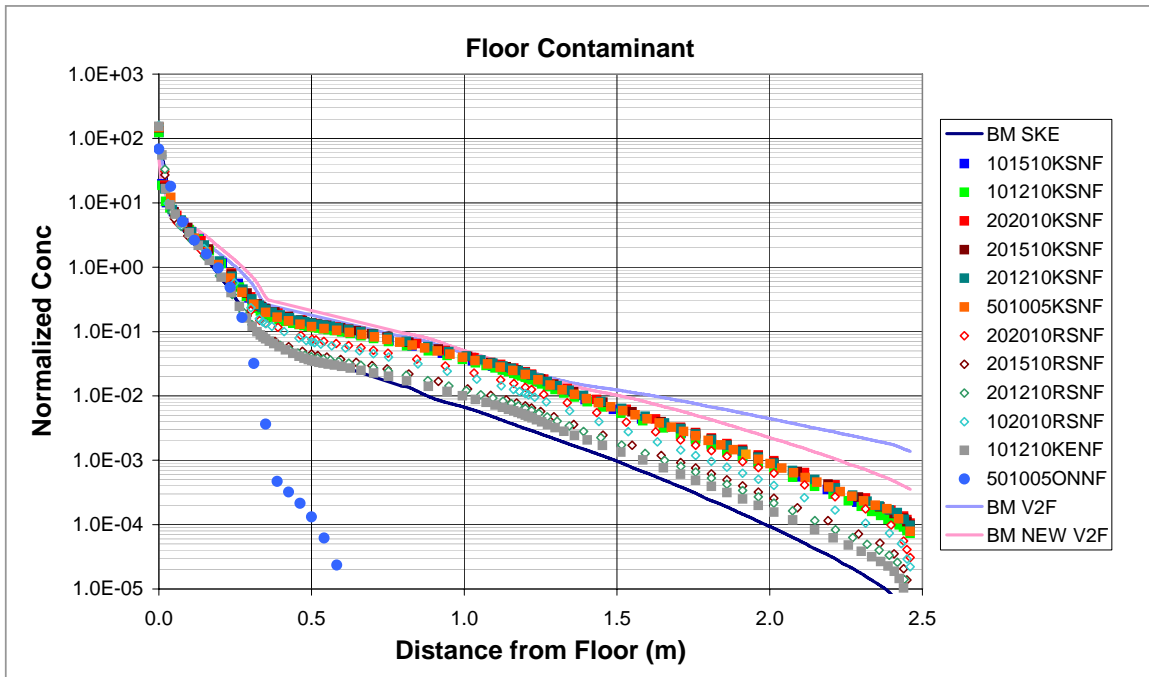
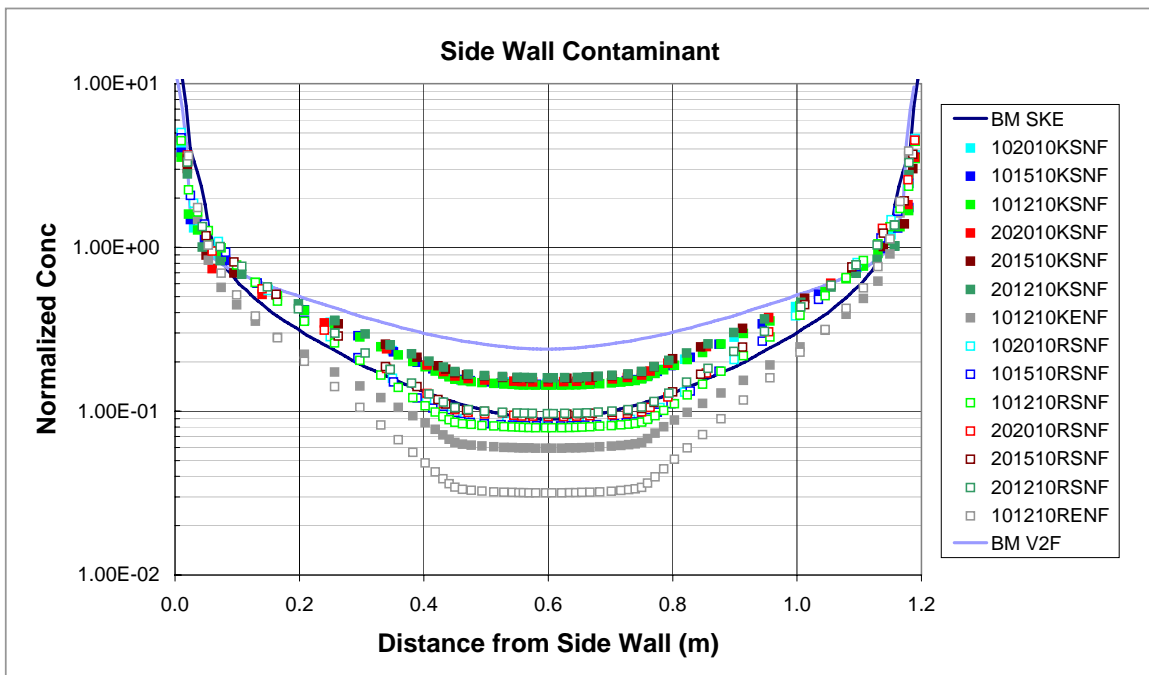


Figure 2. Normalized Concentration of Side-Wall Contaminant at Nose Height



CUBICLE ANALYSIS

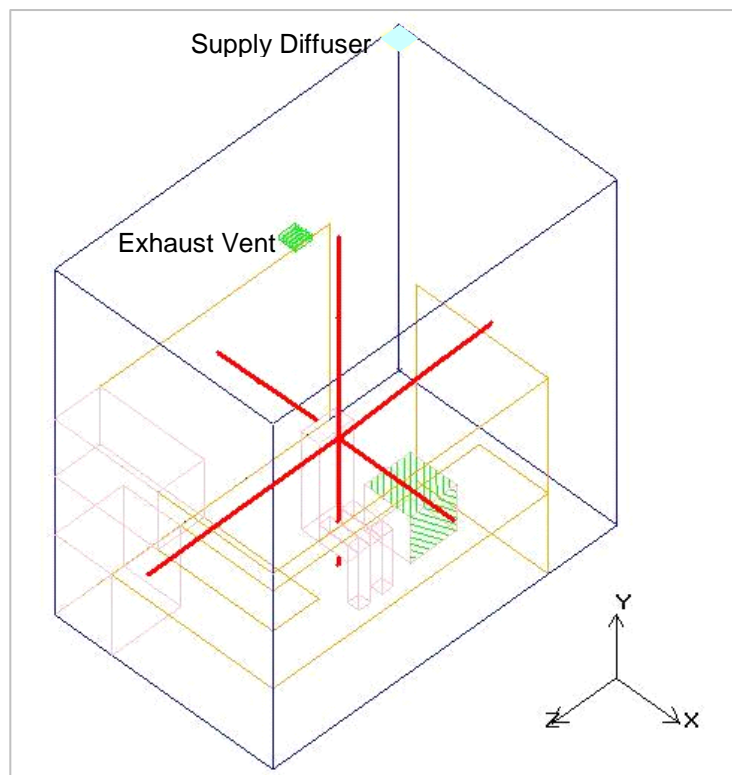
This analysis was carried-out using the simpler, intermediate-grid CFD approach with simplified manikin shapes. This approach is much more manageable, and would point the way for further

refinement in the computational scheme, if needed. We analyzed the concentration field surrounding an occupant in an office cubicle with mixing ventilation. Specifically, we focused on the sensitivity of the BZ contaminant concentrations to 4 geometrical factors likely to exist in a realistic office environment:

- 3 manikin representations: Block (BG), Z-Guy (ZG) and Airpak (AP) manikins,
- 3 supply vent locations: Above the corridor VP1, and at VP2, VP3 and VP4,
- 4 manikin locations: Nominal (N), 0.3 m Back (B), 0.3 m Right (R) and 0.3 m Left (L),
- 2 manikin orientations: Facing computer (F) and facing Wall (W).

The baseline case was a ZG manikin facing the computer (nominal position). Grids for the studied cases were generated in AIRPAK using an initial grid height of 1 cm, a stretch ratio of 2 and a maximum grid size of 10 cm. The $k-\varepsilon$ model with the SWF was employed. Figure 3 depicts the cubicle and a portion of the associated corridor, with a sitting ZG manikin facing the computer. The cubicle has a 1.9x2.4 m floor, 1.7 m partition height and opens to a 0.6 m wide corridor. This cubicle is one of 4 identical adjoining cubicles sharing a ceiling supply diffuser and a corridor with left-right and front-back symmetry. The boundary conditions for the air interface above the panel partitions was one of symmetry. The impervious adiabatic walls also represent planes of temperature and concentration symmetry (no flux across these walls). Therefore, the simulations run here represent one quadrant of the 4-cubicle cluster.

Figure 3. Baseline Cubicle Geometry – Manikin in Nominal Position Facing Computer



The cubicle model incorporates an L-shaped desk, a computer, overhead cabinets, a drawer chest and panel partitions. The floor is carpeted and a computer sits on the long-side of the L-shaped

desk, facing the manikin. A 0.3x0.3 m supply diffuser was placed in the ceiling in such a way as to be shared by 4 cubicles (0.15x0.15 m section for each cubicle). To promote mixing, the diffuser was segmented such that the supply air exits in four directions (x and z, with a discharge angle of 30° downward from horizontal). Each cubicle was equipped with a 0.15x0.15 m discharge vent in the ceiling above the occupant's nominal position. Four emitting sources were represented by surrogate species at a uniform surface mass fraction: carpet, panel partitions desk/cabinets, and computer. In all cases, the computer-cum-monitor was represented as a 0.4x0.4x0.4 m block dissipating 108 W of heat through its surfaces. This block, which was placed 10 cm above the desk facing the manikin with emissions escaping through the top and back of the block.

Effect of Manikin Representation

The first set of CFD simulations were carried out with the three manikin representations placed in the nominal position. The first (BG) was a block 1.25 m high, 0.275 m deep and 0.4 m wide. The surface area of this block was $\sim 1.8 \text{ m}^2$, representing an average male. The second (ZG) was an assembly of blocks forming a torso, thighs, and two legs separated by a 10 cm gap. This manikin was in the seated position and had a total height of 1.25 m and a surface area of $\sim 1.8 \text{ m}^2$. The third (AP) manikin is that of AIRPAK. It is a more elaborate assembly of blocks forming a head, torso, arms, thighs and legs. It is more detailed than the ZG, but much simpler than those in Murakami *et al.*^{8,9,10} and Sideroff *et al.*^{21,22}. The manikins were oriented so that their BZs were all located at the same position, with the manikin's "nose" at 1.2 m above the floor. The diffuser and vent were kept in the baseline location for this set of computations (see Fig. 3). The heat output for all of the manikins was taken as 38 W, representing only the convective sensible part of the heat generated by a person doing normal office activities.

Figure 4 shows the normalized BZ concentrations of contaminants for the various manikin representations. The chart shows that the differences between the various manikin shapes are small (<10%), and that all three manikin representations are exposed to concentrations that are within $\sim 15\%$ of the well-mixed case. Given the small differences resulting from manikin shape, all subsequent analyses were performed with the ZG manikin. This is justified by the fact that the ZG manikin is much simpler than the AP manikin yet it exhibited better agreement with the detailed CFD calculations than the BG manikin, mainly because the separation of the two legs in the ZG manikin allows a more accurate representation of t

Effects Of Supply Vent (Diffuser) Location

Four CFD analyses were performed for the same cubicle with the air supply diffuser placed at each of the four ceiling corners (designated VP1 – VP4) (diffuser) of the cubicle and associated corridor). Here the ZG manikin was placed at the nominal location facing the computer. VP1 is the baseline location used in all the other sensitivity analyses.

Figure 5 presents a summary of the results of these analyses. VP2, which is in the corridor next to the partition leads to higher BZ concentrations for the carpet, desk and panel contaminants (from 10-to-30% higher) than the other vent locations. The best vent position in terms of BZ concentration from a carpet source would be VP4, which is located above the cabinets behind the person. It can also be seen that, with the exception of VP2, which produced higher BZ concentrations for carpet, desk and panel contaminants, the other vent locations produce BZ contaminant concentrations that are within $\pm 10\%$ of the well-mixed case.

Figure 4. Normalized BZ Concentrations for Various Manikin Representations

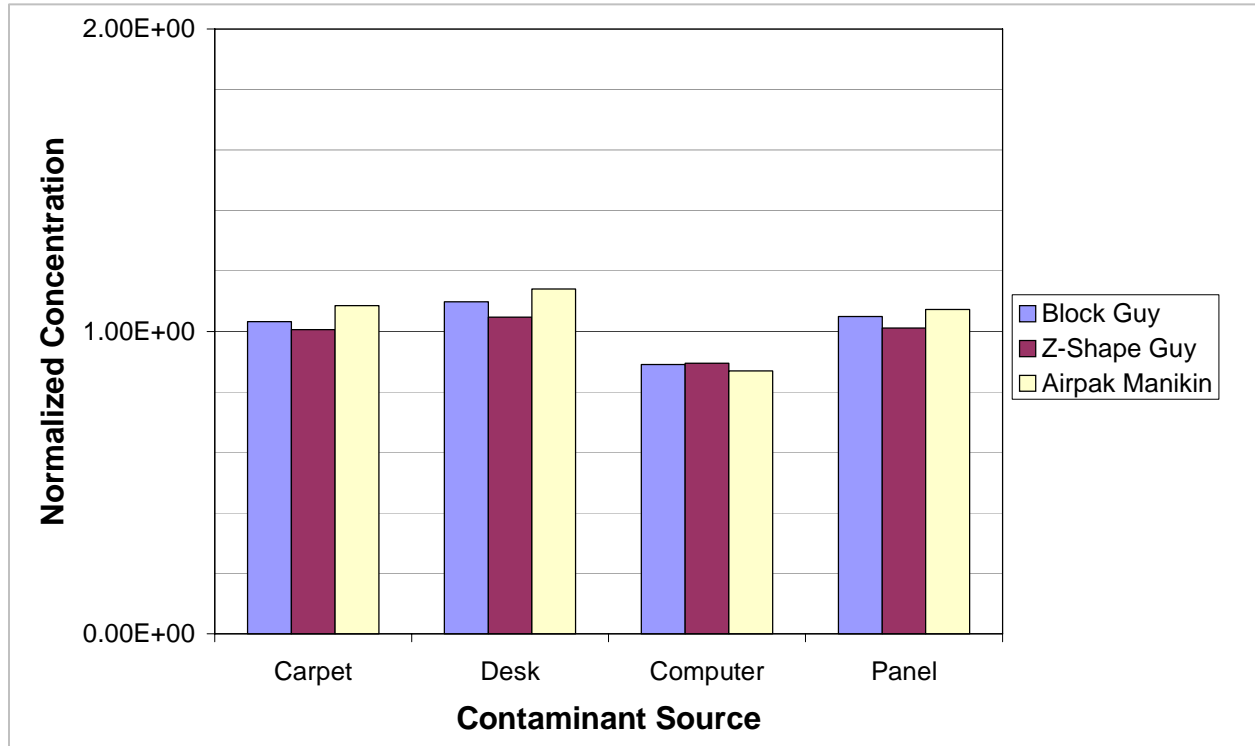
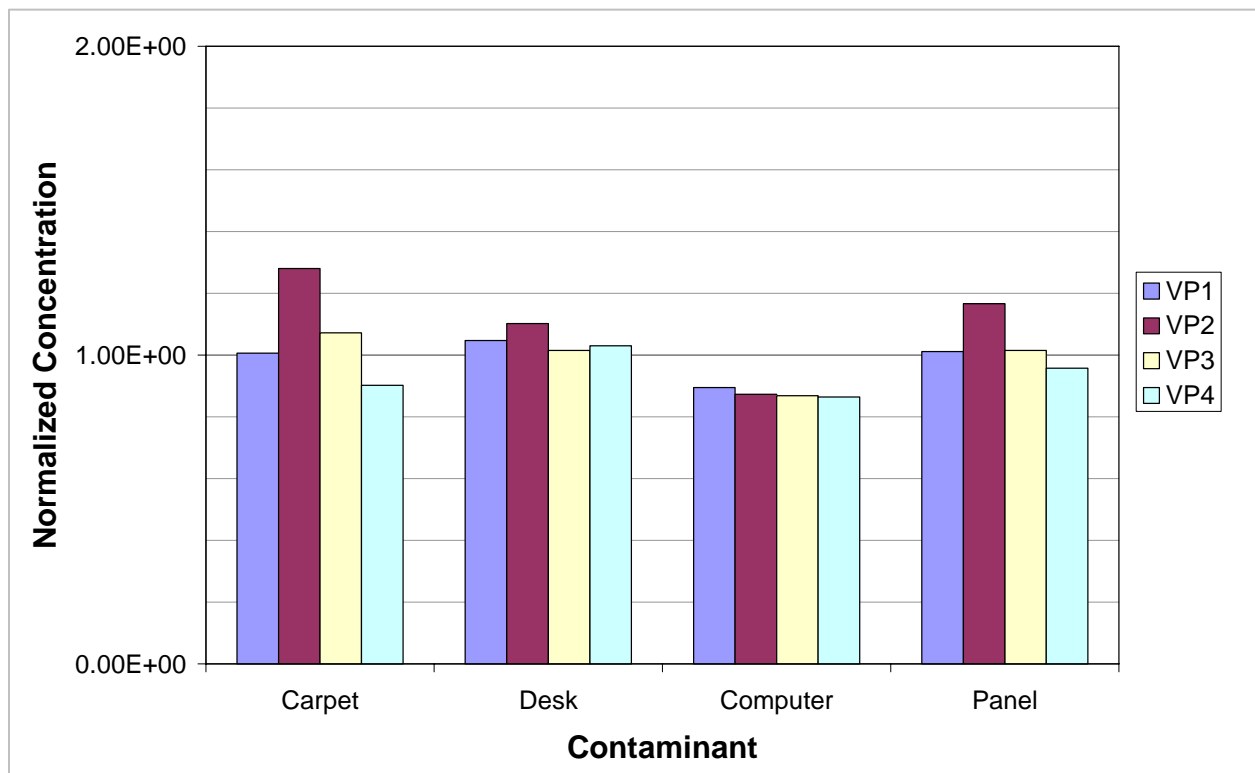


Figure 5. Comparison of the Normalized BZ Concentrations for Various Diffuser Locations

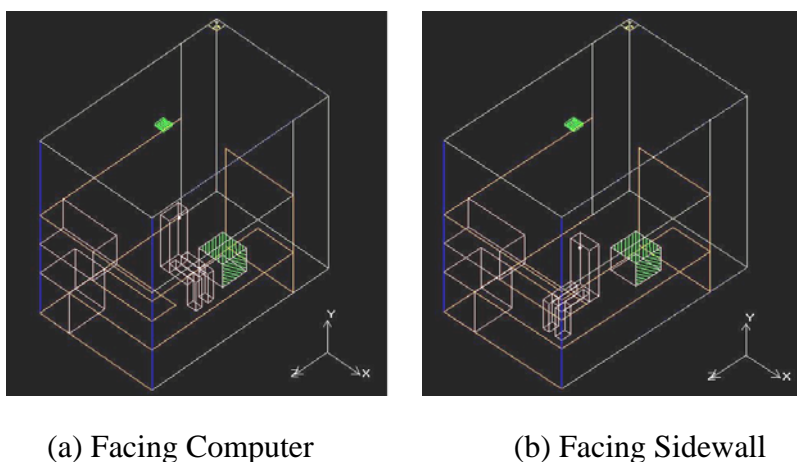


Effect Of Manikin Location and Orientation

Because office occupants do not always stay in the same location facing their computers, we undertook a study of the effect of shifts in the manikin position and orientation on BZ contaminant concentrations. We examined the effect of a 0.3 m (1 ft) shift to the left (LF), right (RF) and back (BF) from the nominal position. We also examined the effect of facing the manikin toward the cubicle side wall (Fig. 6), simulating a person working at his/her desk). In the wall-facing orientation, the manikin was also shifted back (BW), left (LW) and right (RW).

Figure 7 displays the effect of manikin shifts in the forward-facing positions (computer orientation) on the normalized BZ concentrations. It can be seen that these shifts can produce as much as a 20% change in BZ concentration relative to the well-mixed case. The differences in the BZ concentrations for the same contaminant due to these shifts stayed within the $\pm 10\%$ band. Figure 8 displays the effect of manikin shift in the wall-facing positions (desk orientation). It can be seen that the current model predicts higher concentrations for the carpet, desk and panel contaminants while the computer contaminant predicted is lower than the well mixed case. This shows that the well mixed case under-predicts the exposure of the office occupant in the wall-facing position. The largest difference in BZ concentrations is for the carpet contaminant, for which a right shift increases the BZ concentration relative to the well-mixed case by over 40%. This can be explained by the higher concentration located in the corner of the cubicle by the drawer chest, which is then entrained by the person's thermal plume.

Figure 6. Manikin Orientations

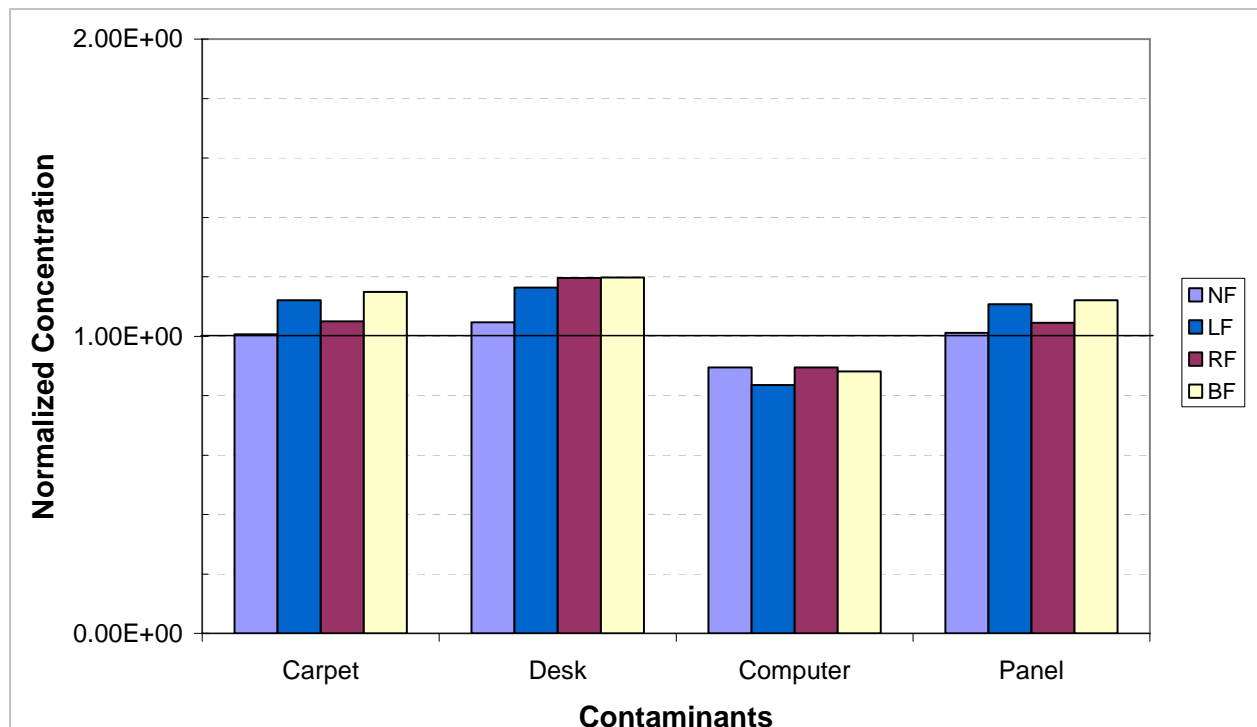


Other Factors

Berrios *et al.*²³ indicate that the number of chemicals emitted from a single source, say a computer or a desk, can be overwhelming. While it is theoretically possible to solve an additional mass conservation partial differential equation for each chemical compound, this is neither practical nor warranted in a CFD analysis of the turbulent transport within a ventilated space. At the low indoor contaminant concentrations, these equations are linear in the concentration. Therefore, the above analysis was conducted with one surrogate contaminant differentiating each of the four sources. In the benchmark comparison, CO₂ was used as the surrogate contaminant; for this analysis, we used SF₆ (panel), toluene (computer), styrene (carpet), and α -pinene (desk), not because they represent the actual emissions, but to

differentiate the various sources in the CFD analysis. It can be argued that when the source boundary condition is defined as a mass flux, changes in grid structure or turbulence model near-wall-treatment will affect only the thin boundary layer. Outside this thin boundary layer, the conditions will be fully turbulent and molecular diffusivity will play a minor role in the prevailing turbulent transport mechanism (for gases, the turbulent Schmidt and Prandtl numbers are nearly constant and close to unity²⁹). Since the exhaust concentration is directly proportional to the emission rate (Eq. 2), one would expect the normalized concentrations to be relatively insensitive to the molecular diffusion coefficients. This was borne out by calculations for the surface contaminants in this study, where a ten-fold variation in the molecular diffusivity had a little or no effect on breathing zone concentrations.

Figure 7. Normalized BZ Concentration for Various Manikin Locations (Facing Forward)

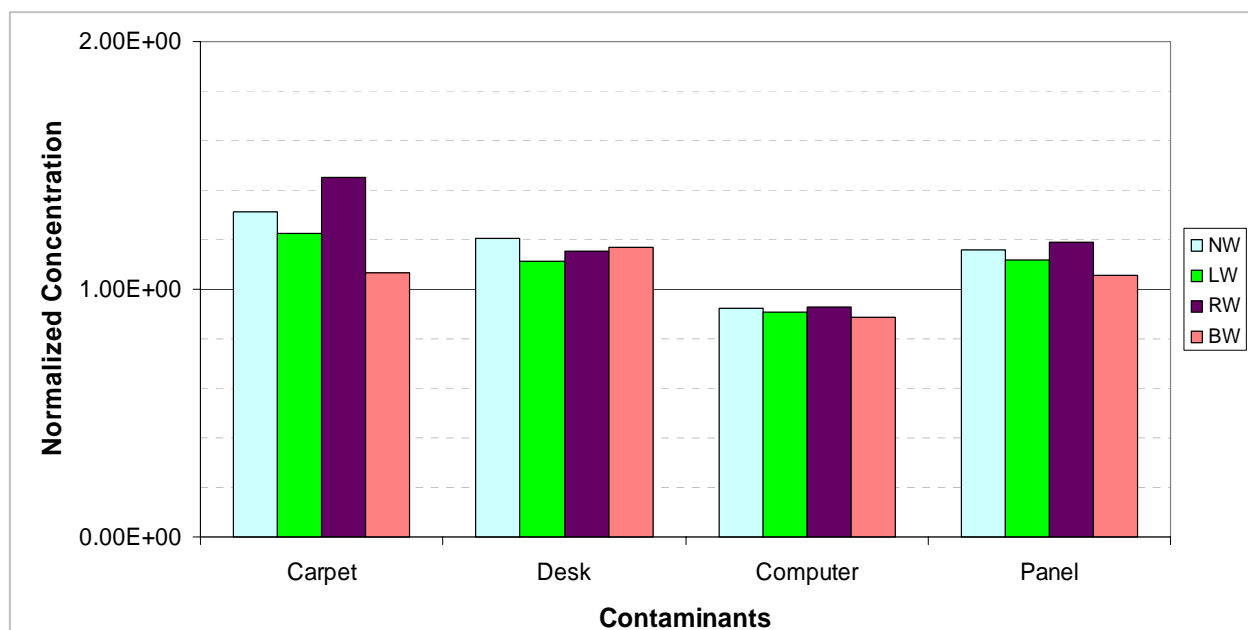


CONCLUSIONS

A CFD model for exposure calculations was developed for an occupant in a typical office cubicle. The model is based on the commercial CFD code AIPAK/FLUENT and the popular and readily accessible $k-\epsilon$ turbulence model. By simplifying the seated occupant representation to an assembly of simple blocks representing the torso, thighs and legs, it was possible to model a realistic cubicle and its occupant with an intermediate grid of $\sim 100,000$ structured cells. This allows the model to run on a single high-end PC, and makes it a practical alternative to the well-mixed zonal models that ignore spatial gradients in the room. This model was compared with a much more refined CFD (millions of unstructured cells) model and was found to predict very similar concentration trends, differing by $\pm 10\%$ at the BZ. The present model was used to study the effect of realistic office cubicle environments with multiple emitting surfaces (e.g., panel partitions, furniture, carpet, computer), and with the occupant in different typical positions. The

present CFD model indicates that the spatial non-uniformities, even in a room ventilated with a mixing-ventilation system, could result in as much as 45%. While the present CFD model is a practical alternative to the much more detailed fine-grid CFD models, and a much more realistic predictor of exposure than the well-mixed zonal models, we expect that the fine-grid models will be needed to predict accurately contaminant concentrations in the BZ when the emission source is within the PME (e.g., pathogens emitted from a sick person, contaminated clothes, or dust resuspended into the PME by human activities). Furthermore, the results of the present model could be used to correct the predictions of the simpler zonal models for spatial non-uniformities, and for the effects of the person's position within the cubicle or the supply diffuser location, allowing a higher fidelity assessment of long-term exposure in the office environment. This model could also be used to study the same effects in offices equipped with displacement or personal ventilation systems, which produce much steeper velocity, temperature and concentration gradients within the occupied spaces.

Figure 8. Normalized BZ Concentration for Various Manikin Locations (Facing Side Wall)



ACKNOWLEDGEMENTS

The work described in this paper was performed under contract No. CR 83104001 awarded by the USEPA to Syracuse University. Dr. Z. Guo, then Mr. B. Henschel were the EPA Project Officers, and under the Faculty Development Program of the NY Office of Science, Technology and Academic Research (NYSTAR).

REFERENCES

1. Sparks, L.E. *EXPOSURE Version 2. A computer mode for analyzing the effects of indoor air pollutant sources on individual exposure*, USEPA NTIS PB91-201095, 1991.
2. Sparks, L.E. *IAQ Model for Windows: RISK Version 1.0.*, USEPA NRMRL, ORD, Research Triangle Park, NC 27711, 1996.

3. Guo, Z. *Environmental Modeling and Software* **2000**, 15(4), 403-410.
4. USEPA, *I-BEAM: Indoor Air Quality – Building Education and Assessment Model*, USEPA Indoor Environments Division, Office of Air and Radiation, EPA 402-C-01-001, 2001.
5. Dols, S.W.; Walton; G.N. and Denton K.R. *CONTAMW 1.0 User Manual: Multizone Airflow and Contaminant Transport Analysis Software*, NISTIR 6476, 2000.
6. Feustel, H.E. and Smith, B.V., Eds. *COMIS 3.0 - User's Guide*, Lawrence Berkeley National Laboratory, Berkeley, CA, 1997.
7. Zhang, J.S.; Shaw, C.Y.; Sander, D.; Zhu, J.P. *MEDB-IAQ: A material emission database and single-zone IAQ simulation program - A tool for building designers, engineers and managers*, CMEIAQ Report 4.2, IRC/NRC, Ottawa, Canada, 1999.
8. Murakami, S, Kato, S., Zeng, J. *ASHRAE Transactions* **1997**, 103(1), 3-15
9. Murakami, S., Kato, S., and Zeng, J. *ASHRAE Transactions* **1998**, 104(2), 226-233.
10. Murakami, S. *Indoor Air* **2004**, 14(7),144-156
11. Nielsen, P.V., Murakami, S., Kato, S., Topp, C. Yang, J-H.. *Benchmarks Test for a Computer Simulated Person*, Aalborg University, Indoor Environmental Engineering, 2003.
12. Nielsen, P.V. *Indoor Air* **2004**, 14(7), 134-143.
13. Topp, C. *Influence of geometry of a computer simulated person on contaminant distribution and personal exposure*, Proceedings of ROOMVENT **2002**, Eight International Conference on Air Distribution in Rooms, Copenhagen Denmark, 2002.
14. Topp, C., Hesselholt, P., Roed, M., Nielsen, P. *Influence of geometry of thermal manikins on room airflow*, Proceeding of Healthy Buildings, Singapore, 2003.
15. Topp, C., Nielsen, P.V and Heiselberg, P. *Indoor Air* **2001**, 11, 162–170.
16. Hayashi, T., Murakami, S., Kato, S., Yang, J.H. *ASHRAE Transactions* **2000**, 108(2), 1173-1178.
17. Hayashi, T., Ishixzu, Y., Kato, S., Murakami, S. *Building and Environment* **2000**, 37, 219-230.
18. Ito. K, Kato S., Zhu Q., Murakami S. *Benchmark Tests for a Computer Simulated Person, CFD Analysis of Chemically Reactive Pollutants in 2D Test Room*, Proceedings of Indoor Air 2002.
19. Oomori, T., Yang, J.H., Kato, S., and Murakami S. *Coupled Simulation of Convection and Radiation on Thermal Environment around an Accurately Shaped Human Body*, Proceedings of ROOMVENT 2004, 9th International Conference on Air Distribution in Rooms, Coimbra, Portugal, 5-8 September, 2004.
20. Versteeg, H.K., Malalasekera, W. *An Introduction to Computational Fluid Dynamics – The Finite Volume Method*, Longman Scientific & Technical, Essex, UK, 1995.
21. Sideroff, C., Dang, T. *Validation and Verification of CFD for the Personal Microenvironment: Benchmark Test for a Computer Simulated Person*, ROOMVENT 2004, 9th International Conference on Air Distribution in Rooms, Coimbra, Portugal, September 5-8, 2004.

22. Sideroff, C.N. and Dang, T.Q. *CFD Analysis of the Flow around a Computer Simulated Person in a Displacement Ventilated Room*, Proceedings of Indoor Air **2005**, Beijing, China.
23. Berrios, I., Zhang, J>S, Guo, B., Smith, J., and Zhang, Z. *Volatile Organic Compounds (VOCs) Emissions from Sources in Partitioned Office Environment and Their Impact on IAQ*, Proceedings of Indoor Air 2005, 2064-2069, 2005.
24. Fluent Inc., Fluent 6.1 User's Guide (www.fluent.com), See also <http://airpak.fluent.com/>.
25. Chen, Q., Weiran, X. *Energy and Buildings* **1998**, 28 137-144
26. Hu, B., He, G.Q., J. Srebric, J. and Yang, X.D. *The influence of contaminant source area on CFD simulations for indoor point sources*, Proceedings of Indoor Air 2005, 2882-2886, 2005.
27. He, G., Yang, X. and Srebric, J. *ASHRAE Transactions* **2005**, (OR-05-5-5).
28. Novoselac, A., Srebric, J. *ASHRAE Transaction* **2003**, (KC-03-4-5).
29. Kays, W. M., and Crawford, M.E. *Convective Heat and Mass Transfer – 3rd Ed*, McGraw Hill, Inc., New York, 1993.